

Soft tunable diffractive optics with multifunctional transparent electrodes enabling integrated actuation

Xiaobin Ji^{a)}, Samuel Rosset and Herbert R. Shea^{b)}

Microsystems for Space Technologies Laboratory, École Polytechnique Fédérale de Lausanne (EPFL), 2002 Neuchâtel, Switzerland

We present a stretchable tunable transmission grating in which the optical surface serves simultaneously as an electrode for electrostatic actuation. Tunable optics based on elastomers allow for a large tuning range, but integrating an actuator generally significantly increases device footprint. By combining optical and electrical functions into one multifunctional transparent material, we use here the grating as an integral part of a Dielectric Elastomer Actuator, and hence avoid placing actuators around the grating. The grating/electrode consists of a 750 nm thick soft ionogel, which is bonded on both sides of a 13 μm thick silicone membrane. The top ionogel electrode is corrugated (2 μm pitch) and serves as the diffraction grating. The bottom electrode is planar. Applying a voltage between the electrodes generates a Maxwell pressure, leading to in-plane expansion of the elastomer and electrodes. Linear actuation strain of 12.8% is obtained at 1300 V. The ionogel grating maintains accurately its period after 500 cycles and after one-month storage. The ionogel electrodes present self-clearing properties, allowing operation of the actuator close to the breakdown voltage. This device presents an unprecedented level of integration by making accurate grating structures directly on a transparent soft ionogel conductor, which opens broad possibilities for making tunable optics.

Soft but accurately deformable optical elements such as tunable lenses and gratings enable dynamically changing optical properties without requiring the translation of rigid elements. Examples of flexible tunable optics in biology include the human eye where the crystalline lens is deformed by the annular ciliary muscle and the grating structures on butterfly wings.¹

Man-made soft tunable optics generally consist of a deformable optical element, often based on an elastomer, and an external actuator. We report here on a method to integrate a compliant electrostatic actuator and a stretchable grating into a single multifunctional elastomer material by accurately molding transparent soft conductive ionogel into an optical grating (or any diffractive optics)

Tunable gratings find applications today in many fields, including spectroscopy,² projection displays,³ and telecommunication applications.⁴ Integrating the actuator with the optical elements allows for much greater compactness, higher performance and higher efficiency than using an external actuator. Using a soft actuator enables for instance integration in soft robotics and in wearable applications.

Of the many miniaturized actuation mechanisms suitable for tunable optics (e.g. piezoelectric⁵, electrostatic⁶, thermal⁷, electromagnetic⁸, pneumatic⁹), dielectric elastomer actuators (DEAs) are particularly appealing for tunable optics in view of their compliance, very high strain, and high energy density.¹⁰ We present here a method to use the DEA as the transparent grating, thus creating a tunable grating where the actuator adds negligible complexity or mass to the device. As DEAs are stretchable and soft, using them to drive elastomer-based optics can allow integrating or embedding of tunable gratings into complex shapes or flexible systems.

DEAs have been used to drive tunable lenses¹¹⁻¹³ as well as to tune the period of optical gratings.¹⁴⁻¹⁶ DEAs consist of a dielectric elastomer film (usually silicones¹⁷ or acrylics¹⁰) sandwiched between two stretchable electrodes. When a voltage difference is applied between the electrodes, the dielectric film is compressed by the electrostatic pressure (Maxwell pressure) generated by the electrical charges on the electrodes. The membrane decreases in thickness and expands in plane.¹⁸⁻²⁰ This mechanism of actuation provides large actuation strain (over 200%²¹), fast response time and potentially high efficiency, which distinguishes dielectric elastomers from other electrostrictive polymers.¹⁰

DEA-based tunable gratings generally consist of two components: a) a DEA composed of a thin elastomer membrane stretched on a frame with patterned compliant electrodes. b) a soft grating replicated in silicone, bonded on the stretched membrane and deformed by the expansion of the DEA electrodes (see Fig. 1a). Adding the grating on the DEA reduces the maximum achievable strain, since the device becomes stiffer. The stiffening effect is even more pronounced if the grating is metallized to increase reflectivity.

One solution to improve the tuning range of a DEA-driven grating is to avoid adding the grating layer. Zhao et al.²² reported a tunable grating controlled by DEAs with one electrode patterned as a grating. However the electrodes are opaque so the grating must be used in reflection, which limits applications.²³ While transparent compliant electrodes for DEAs based on hydrogels,²⁴ ionogels,²⁵ CNT^{11,21} and silver nanowires²⁶ have been reported, these electrodes have not been patterned into gratings.

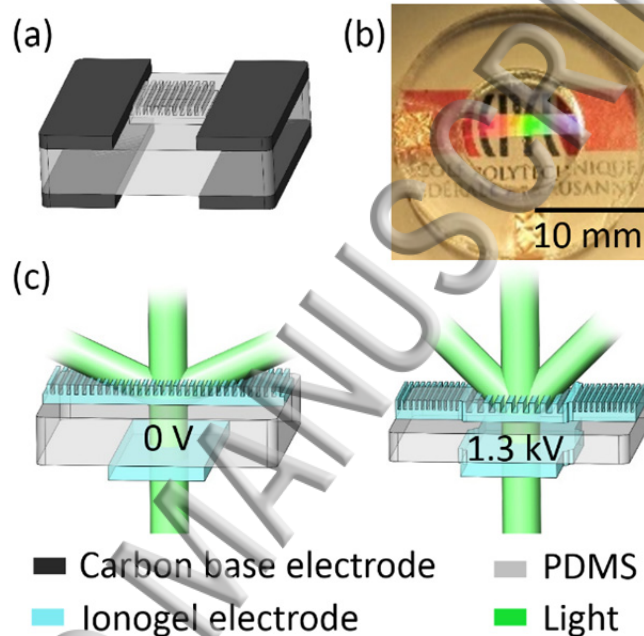


FIG. 1. (a) Conventional configuration of a Dielectric Elastomer Actuator (DEA) -based tunable grating consisting of a central grating bonded on a membrane compressed by the expansion of the DEA placed on the periphery; (b) Photograph of our tunable grating in which a central DEA electrode also serves as the stretchable grating; (c) Operating principle of our tunable grating: The transparent central grating is molded directly in the top ionogel electrode of a DEA. The transparent bottom ionogel electrode is on the other side of a 13 μm thick PDMS membrane. When a voltage is applied between the two electrodes, the membrane expands in plane, increasing the grating period.

In this paper, we report a tunable transmission grating that is an integral part of a DEA using transparent ionogel electrodes. The upper DEA electrode has a corrugated surface and acts both as a soft tunable grating and as the electrode of the actuator (Fig. 1b, 1c). No additional layer is therefore required on or next to the DEA, i.e. there is no additional layer that increases stiffness. The entire device is transparent, so that it can be used in transmission. The fabrication process of the tunable grating is simplified thanks to a reduced number of fabrication steps. The transparent deformable

electrode is used as a diffractive element with μm -scale periodic features. We thus combine intrinsic electric and optical functions in one transparent material, opening exciting possibilities for tunable optics.

Our complete device (shown in Fig. 1b) has a circular shape, with a diameter of 10 mm. The outline dimensions of the ionogel electrodes are 2 mm x 10 mm. The two electrodes are placed orthogonally on each side of the membrane (Fig. 1c). The active grating zone of dimension 2 mm x 2 mm is therefore at the center of the PDMS membrane, where the top and bottom electrodes overlap. The overall DEA active zone dimensions were chosen such that the passive zone is large enough to not negatively impact the strain of the DEAs.²⁷ The unactuated pitch of the grating-shaped electrode is 2 μm , designed for use with visible light.

A Poly(methyl methacrylate) (PMMA) based ionogel was chosen for the electrode as it combines high optical transparency, very low haze, sufficient electrical conductivity, low stiffness, the ability to be molded into a grating structure with nm-accuracy, and provides good adhesion to silicone membranes. An imidazolium-based ionic liquid was used as the plasticizer²⁸ thus allowing the formation of a soft ionogel. We measured over 93.0% transmittance for wavelengths between 500 nm and 1600 nm for a 700 nm thick ionogel film on a 20 μm thick PDMS membrane, compared with over 94.1% transmittance for the PDMS membrane alone. The scattered light intensity is 1.2% and 1.0% in the same wavelength range for the two samples. The ionogel electrodes thus introduce negligible haze and show excellent transparency.

The ionogel solution is formed by adding 0.4 g of PMMA, 1.2 g ionic liquid EMITCM ((1-Ethyl-3-methylimidazolium tricyanomethanide), io-li-tec, IL-0316-HP-0050) and 10 g of acetone into a 25 ml glass bottle with cover, and stirred for 5 h at 45 °C. The solution is cooled to room temperature, and is then ready for casting transparent ionogel electrodes.

For the electrode used as the grating, the solution is applied by blade casting on a commercial plastic

grating master purchased from Edmund Optics (6 x 12 inches, 500 grooves/mm), using an applicator with a gap of 25 μm . For the smooth bottom electrode, the solution is blade casted on flat Polyethylene terephthalate (PET) substrate (Melinex ST-506, DuPont Teijin Films), using a gap of 25 μm to obtain a final thickness of 750 nm after solvent evaporation. After casting, the ionogel sheets are placed in an oven at 80 $^{\circ}\text{C}$ for 2 hours. Once dry, they are cut into 2 mm x 40 mm strips.

The PDMS membrane is fabricated following the process described by Rosset et al.²⁹ A PDMS solution consisting of Sylgard 186 (Dow Corning) part A (45.5% wt) and part B (4.5% wt) diluted in the siloxane solvent OS-2 (Dow Corning) (50% wt) is blade casted on a PET substrate coated with a poly(acrylic acid) (PAA) sacrificial layer, and then cured at 100 $^{\circ}\text{C}$ for 1h (Fig. 2a). By dissolving the PAA sacrificial layer, a suspended PDMS membrane is obtained. The PDMS membrane is equibiaxially pre-stretched with a lateral ratio of $\lambda = 1.3$, and fixed to a circular PMMA membrane holder with an adhesive layer. The pre-stretched PDMS membrane has a thickness of 13 μm (Fig. 2b).

The corrugated grating electrode is bonded on the PDMS membrane (Fig. 2c), and the grating master is then carefully peeled off (Fig. 2d). Next, the flat bottom electrode is applied on the other side of the PDMS membrane, oriented perpendicular to the corrugated grating electrode (Fig. 2e). The PET substrate of the bottom ionogel electrodes is peeled off (Fig. 2f). Finally, the device is fixed on a PMMA circular holder with copper contacts.

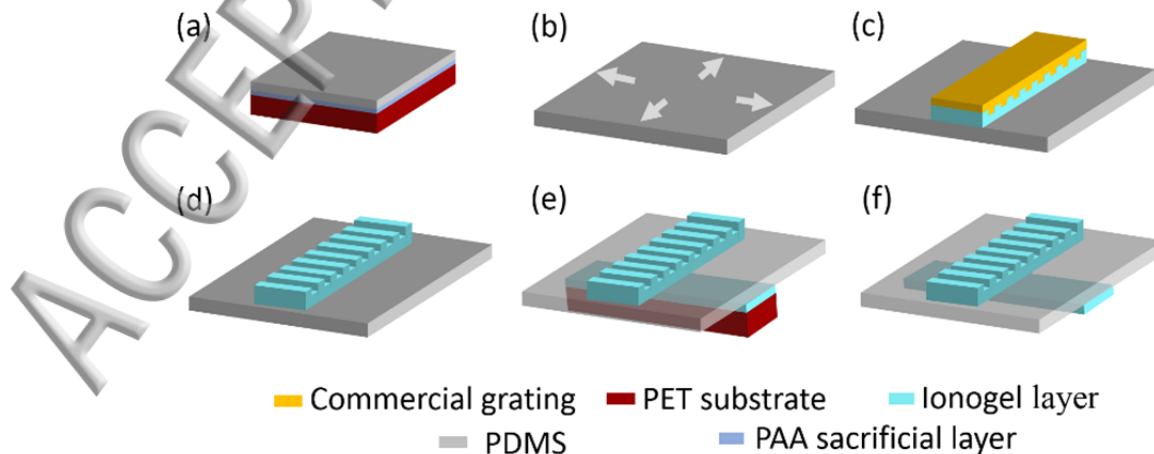


FIG. 2. Transparent DEAs fabrication process flow. (a) Casting PAA sacrificial layer and PDMS layer on a PET substrate. (b) Release of the PDMS layer by dissolving the PAA sacrificial layer in hot water. Followed by prestretching of the suspended PDMS membrane with a stretch ratio of 1.3. (c) Application of the top ionogel electrode, which has been casted on a commercial plastic grating master. (d) Peeling off of the master grating from the top electrode. (e) Application of the flat bottom electrode. (f) Peeling off the PET substrate from the flat electrode, then attach the device to a PMMA holder.

The first-order diffraction angle θ_1 of the tunable grating is given by the well-known equation³⁰:

$$\sin(\theta_1) = \frac{\lambda}{d} \quad (1)$$

with λ the wavelength of the incident light and d the period of the grating. When a voltage difference is applied between the two electrodes, the PDMS is squeezed and expands in area. Since the electrodes are bonded to the elastomer membrane, they expand with it. Consequently, the period of the grating d can be tuned by the applied voltage V . For DEAs with small deformation, the lateral strain S_x is given by³¹:

$$S_x = \frac{1}{2} \frac{\epsilon}{Y t^2} V^2 = b V^2 \quad (2)$$

with ϵ is the permittivity, Y the Young's modulus, and t is the thickness of the dielectric membrane; V is the applied voltage. The grating period thus depends on the applied voltage as:

$$d = d_0 (1 + b V^2) \quad (3)$$

with d_0 the initial period of the grating (nominally 2 μm in our case). The first diffraction angle can be calculated by combining Eq. (1) and Eq. (3):

$$\theta_1 = \arcsin\left(\frac{\lambda}{d_0(1+bV^2)}\right) \quad (4)$$

For simplicity, we have assumed that the electrodes are perfectly compliant and have no impact on the actuator strain. This is an acceptable hypothesis in this case³², given that the electrodes are much thinner than the dielectric layer.

The electrode material properties and the performance of the devices were measured. The ionogel electrodes have a Young's modulus of 192 ± 4 kPa (using an Instron Pull-tester). The thickness of the smooth bottom electrode is 750 nm, measured by white light interferometry (Veeco Wyko NT1100).

The sheet resistance of this electrode is approximately $700 \text{ k}\Omega/\square$. The grating-shaped electrode has a maximum thickness of 750 nm and an approximately 400 nm deep grooves. Because the grating/electrode is made of a soft ionogel material, we considered the possibility that the ionogel might flow with time, reducing the amplitude and accuracy of the grating. To investigate this, the profile of the grating electrode was measured as a function of time and of actuation cycles (Fig. 3). The period of the grating electrode remains extremely stable over the two weeks and 500 actuation cycles, about $1.92 \mu\text{m}$. The grating height does not significantly change within 500 actuation cycles. The height decreases however by about 90 nm after one week, and by another 40 nm in the second week of storage. To directly see the effect of change in grating profile on optical performance, images of the diffraction patterns were recorded immediately after fabrication, after one week of storage and after two weeks of storage (Fig.4). A decrease in grating efficiency over time is observed, and the degradation is accelerated by exposure to laser light.

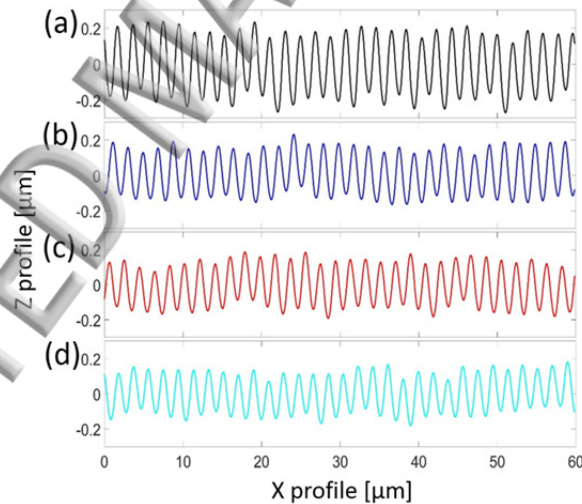


FIG 3. Height profile of the ionogel grating. (a) after fabrication. (b) after one week of storage. (c) after one week of storage followed by 500 actuation cycles. (d) After one additional week of storage. The grating period is unchanged, though the grating height decreases slightly.

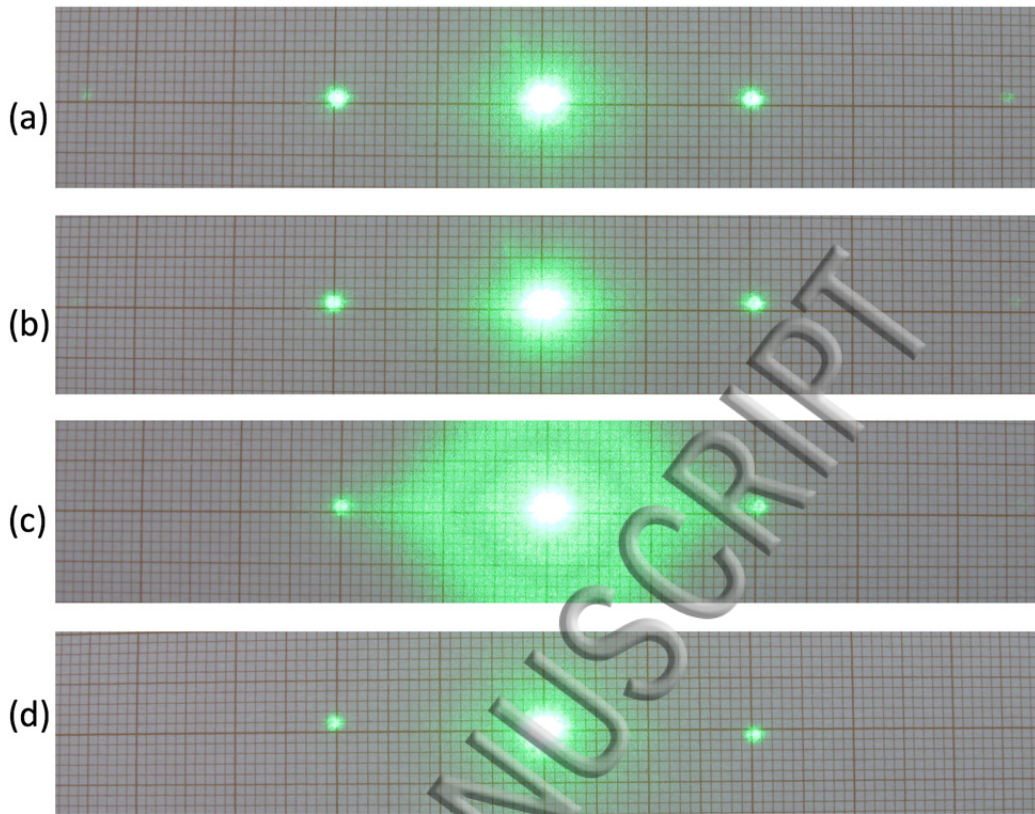


FIG 4. Diffraction patterns of an ionogel grating: (a) immediately after grating fabrication, (b) one week later, and (c) two weeks later. (d) Diffraction pattern after 2 weeks storage of an ionogel grating made at the same time as the one in 4a but that did not experience daily exposure to the laser. The diffraction efficiency decreased with time, and does so much more rapidly when exposed to the laser.

The DEAs with ionogel electrodes are driven by a 100 Hz bipolar square signal. Ion diffusion from the electrodes into the PDMS membrane under DC voltages led to a slow drift in actuated position, so AC actuation was chosen, which allowed for stable multi-hour continuous operation. The grating strain vs. voltage curves are plotted in Fig. 5a. The loading data shows the typical V^2 strain dependence expected for DEA in the small displacement case. At 1.3 kV actuation voltage, 12.8% linear strain is obtained. Fig. 5b plots the strain vs. time after a 1 kV voltage step. 7% strain is reached within 1 s, and then remains constant thereafter for over 1000 s (when we stopped the experiment).

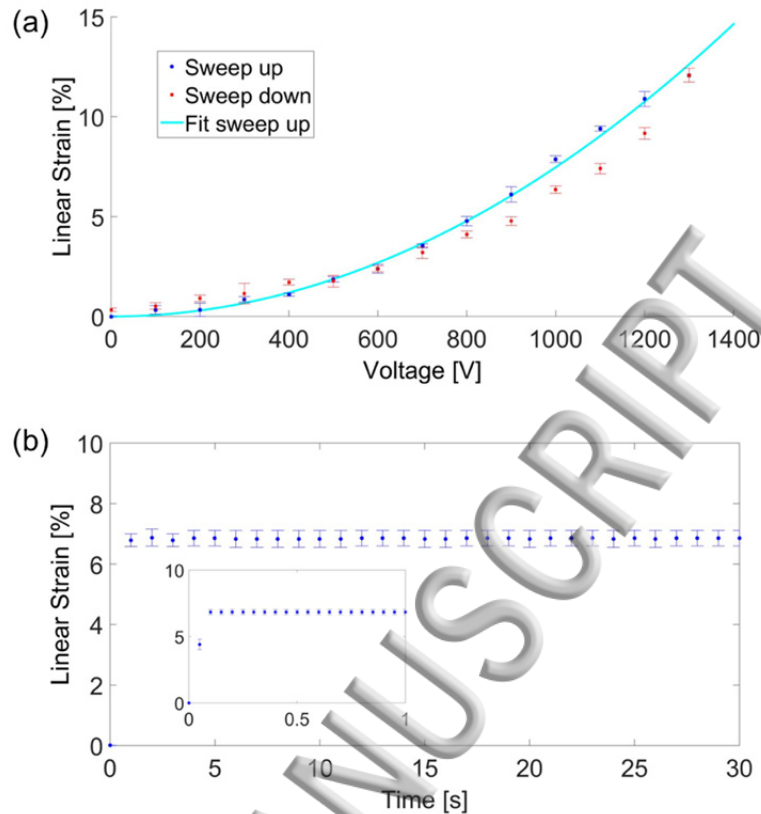


FIG. 5. (a) Actuation strain generated as a function of the AC voltage (at 100 Hz) applied to the DEAs device. Strain is measured during loading and unloading, with 20 s interval between points. (b) Strain as a function of time for a fixed AC voltage amplitude of 1 kV. Inset: zoom between 0 and 1 showing stabilization within 100 ms.

When the electric field applied across the membrane becomes too large, dielectric breakdown occurs. This is a major failure mode for DEAs.¹⁷ With our ionogel electrodes, when dielectric breakdown occurs, the heat generated by the leakage current locally vaporizes the electrode around the failure point, thus stopping the current flow and allowing the DEA to continue operating. DEAs with this ionogel electrodes present the property of self-clearing,²¹ allowing extended operation very close to the breakdown voltage.

The change of the first diffraction angle was recorded as a function of the drive voltage. The tunable grating is placed 79.5 mm from a screen. Laser light with a wavelength of 532 nm is shone through the center of the tunable grating actuators. Several diffraction orders are recorded with a camera as the voltage is swept. The distance between the first diffraction laser spot and the principle one, noted as D

(mm), is measured by using the software ImageJ [ImageJ-win64, <http://imagej.net/Fiji>]. The first diffraction angle, θ_1 (degree), can then easily be calculated by Eq. (5):

$$\theta_1 = \arctan\left(\frac{D}{79.5}\right) \quad (5)$$

θ_1 vs. applied voltages is plotted on Fig. 6, together with the simple theoretical model, Eq. (4). The first diffraction angle changing from 15.67° at 0 V to 14.25° at 1.3 kV, leading to a tuning range of 1.42° . A fit of Eq. (4) on the experimental data leads to a d_0 of $1.965 \mu\text{m}$, which is very close to the value from measurement ($1.92 \mu\text{m}$). An excellent agreement is found between the theoretical model and the figure based on the experimental data points.

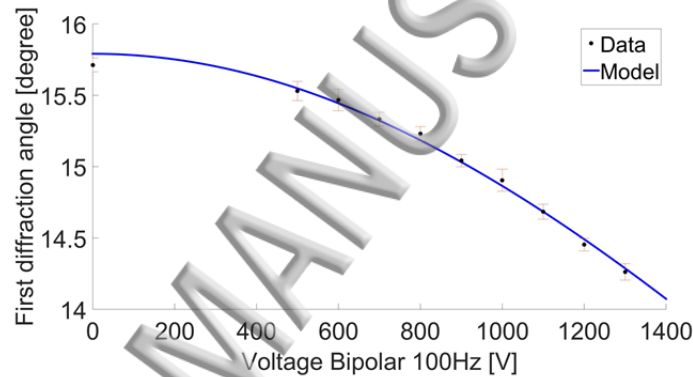


FIG. 6. First diffraction angle as a function of the drive voltage. The model of Eq. (4) shows very good agreement with the data using an initial grating pitch of $1.965 \mu\text{m}$.

In summary, we have shown that soft ionogels can be integrated into DEA-based optical devices to play the dual role of transparent electrode and tunable diffractive optical element. DEAs usually have black light-absorbing electrodes,³³ which greatly limits their use for optical devices. Our soft transparent electrodes enable configurations in which light passes through the deformable actuators, which can be accurately patterned as diffractive optical elements. Up to 12.8% change in grating period is obtained with our prototype, and a larger tuning range could be achieved by optimizing the device. In addition to the transparency, the self-clearing properties of the ionogel electrodes can increase the lifetime of the actuator, as it makes dielectric breakdown events non-destructive for the device. In addition to gratings, these ionogel electrodes can be applied to other optical applications actuated by

IDEAs, such as tunable lenses in configurations where the electrodes are in the light path, molding the electrodes to provide combined optical and electrical function.

^{a)} xiaobin.ji@epfl.ch

^{b)} herbert.shea@epfl.ch

This work was partially funded by the European Union's Horizon 2020 research and innovation programme under the Marie Skłodowska-Curie grant agreement No 641822 - MICACT via the Swiss State Secretariat for Education, Research and Innovation. The authors warmly thank M. Imboden, N. Besse and S. Schlatter for their help with fabrication and characterization.

¹K. Watanabe, T. Hoshino, K. Kanda, Y. Haruyama, S. Matsui, *Jpn. J. Appl. Phys.* **44**, L48 (2005).

²S. C. Truxal, K. Kurabayashi, Y. C. Tung, *International Journal of Optomechatronics* **2**, 75 (2008).

³Z. Jie, Z. Yong, S. Jiyong, W. Ning, W. Wei, *Applied Optics* **48**, 9 (2009).

⁴A. Kocabas, A. Aydinli, *Opt. Express* **14**, 22 (2006).

⁵C. W. Wong, Y. Jeon, G. Barbastathis, S. G. Kim, *Journal of Microelectromechanical Systems*. **13**, 6 (2004).

⁶X. Li, C. Antoine, D. Lee, J. S. Wang, O. Solgaard, *Journal of Microelectromechanical Systems*. **15**, 3 (2006).

⁷Y. S. Yang, Y. H. Lin, Y. C. Hu, C. H. Liu, *J. Micromech. Microeng.* **19**, 015001 (2009).

⁸H. Yu, G. Zhou, F. S. Chau, S. K. Sinha, *Sensors and Actuators A* **167**, 602 (2011).

⁹N. T. Nguyen, *Biomicrofluidics* **4**, 031501 (2010).

¹⁰R. Pehrine, R. Kornbluh, Q. Pei, J. Joseph, *Science* **287**, 836 (2000).

¹¹S. Shian, R. M. Diebold, D. R. Clarke, *Opt. Express* **21**, 7 (2013).

¹²F. Carpi, G. Frediani, S. Turco, D. D. Rossi, *Adv. Funct. Mater.* **21**, 4152 (2011).

¹³L. Maffli, S. Rosset, M. Ghilardi, F. Carpi, H. R. Shea, *Adv. Funct. Mater.* **25**, 1656 (2015).

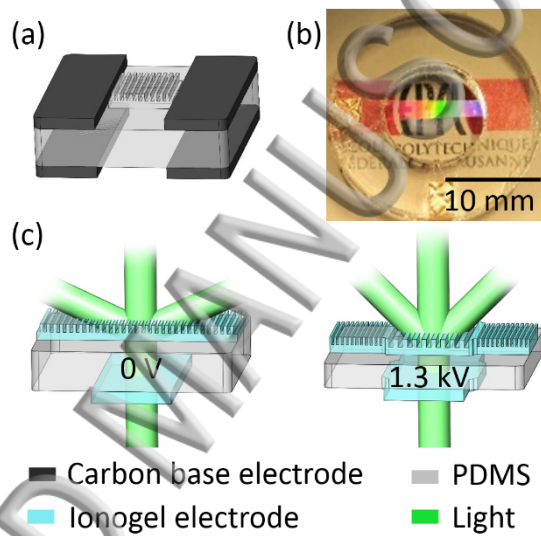
- ¹⁴M. Aschwanden, M. Beck, A. Stemmer, IEEE Photonics Technology Letters **19**, 14 (2007).
- ¹⁵M. Kollosche, S. Döring, J. Stumpe, G. Kofod, Optics Letters **36**, 8 (2011).
- ¹⁶M. B. Krishnan, S. Rosset, S. Bhattacharya, H. R. Shea, Optical Engineering **55**, 4 (2016).
- ¹⁷F. B. Madsen, A. E. Daugaard, S. Hvilsted, A. L. Skov, Macromol. Rapid Commun. **37**, 378 (2016).
- ¹⁸F. Carpi, I. Anderson, S. Bauer, G. Frediani, G. Gallone, M. Gei, C. Graaf, C. Jean-Mistral, W. Kaal, G. Kofod, M. Kollosche, R. Kornbluh, B. Lassen, M. Matysek, S. Michel, S. Nowak, B. O'Brien, Q. Pei, R. Pelrine, B. Rechenbach, S. Rosset, H. R. Shea, Smart Mater. Struct. **24**, 105025 (2015).
- ¹⁹I. A. Anderson, T. A. Gisby, T. G. McKay, B. M. O'Brien, E. P. Calius, Journal of Applied Physics **112**, 041101 (2012).
- ²⁰P. Brochu, Q. Pei, Macromol. Rapid Commun. **31**, 10 (2010).
- ²¹W. Yuan, L. Hu, Z. Yu, T. Lam, J. Biggs, S. M. Ha, D. Xi, B. Chen, M. K. Senesky, G. Grüner, Q. Pei, Adv. Mater. **20**, 621 (2008).
- ²²Z. H. Fang, C. Punckt, E. Y. Leung, H. C. Schniepp, I. A. Aksay, Applied Optics **49**, 35 (2010).
- ²³T. Rasmussen, The benefits of transmission grating based spectroscopy, Ibsen Photonics (2010).
- ²⁴C. Keplinger, J. Y. Sun, C. C. Foo, P. Rothmund, G. M. Whitesides, Z. Suo, Science **341**, 984 (2013).
- ²⁵B. Chen, J. Lu, C. H. Yang, J. H. Yang, J. Zhou, Y. M. Chen, Z. Suo, ACS Appl. Mater. Interfaces **6**, 7840 (2014).
- ²⁶J. Liang, L. Li, D. Chen, T. Hajagos, Z. Ren, S. Y. Chou, W. Hu, Q. Pei, Nature Communications **6**, 7647 (2015).
- ²⁷S. Rosset, O. A. Araromi, H. R. Shea, Extreme Mechanics Letters **3**, 72 (2015).
- ²⁸M. P. Scott, M. Rahman, C. S. Brazel, European Polymer Journal **39**, 1947 (2003).
- ²⁹S. Rosset, O. A. Araromi, S. Schlatter, H. R. Shea, J. Vis. Exp. **108**, e53423 (2016).
- ³⁰C. Palmer, E. Loewen, *Diffraction grating handbook* (Newport Corporation, 2005) p.24.

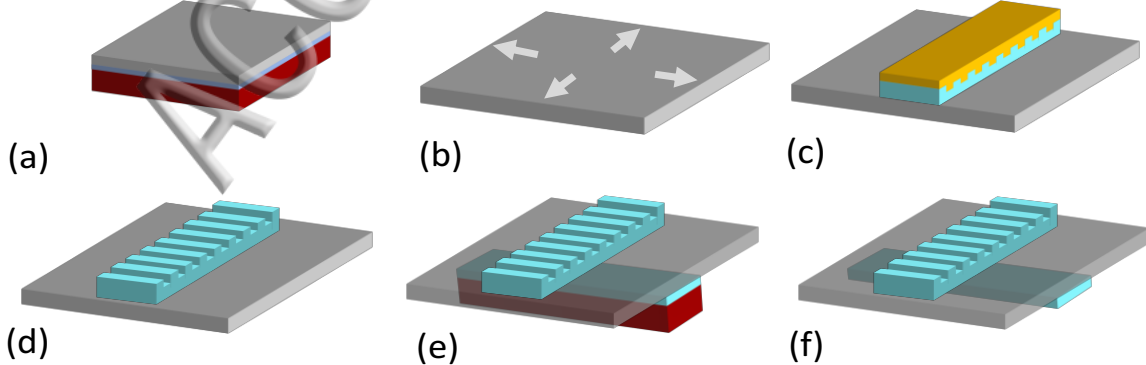
³R. E. Pelrine, R. D. Kornbluh, J. P. Joseph, Sensors and Actuators A **64**, 77 (1998).

³²A. Poulin, S. Rosset, H. R. Shea. Applied Physics Letters **107**, 244104 (2015).

³³S. Rosset, H. R. Shea, Appl Phys A **110**, 281 (2013).

ACCEPTED MANUSCRIPT

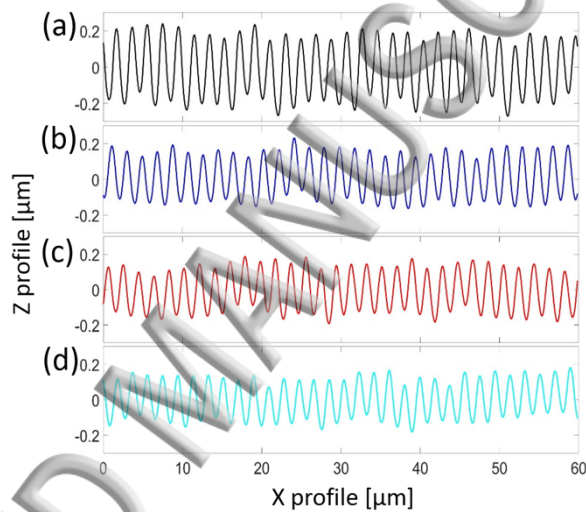




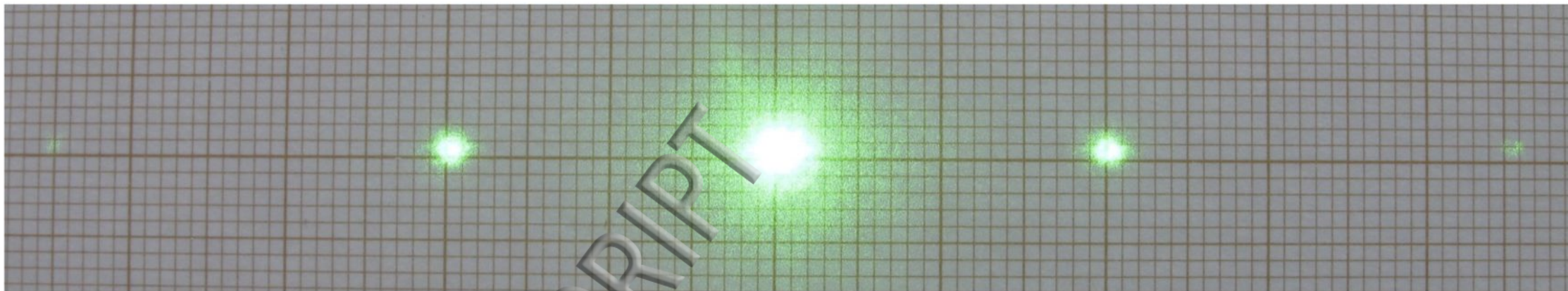
Commercial grating
PDMS

PET substrate

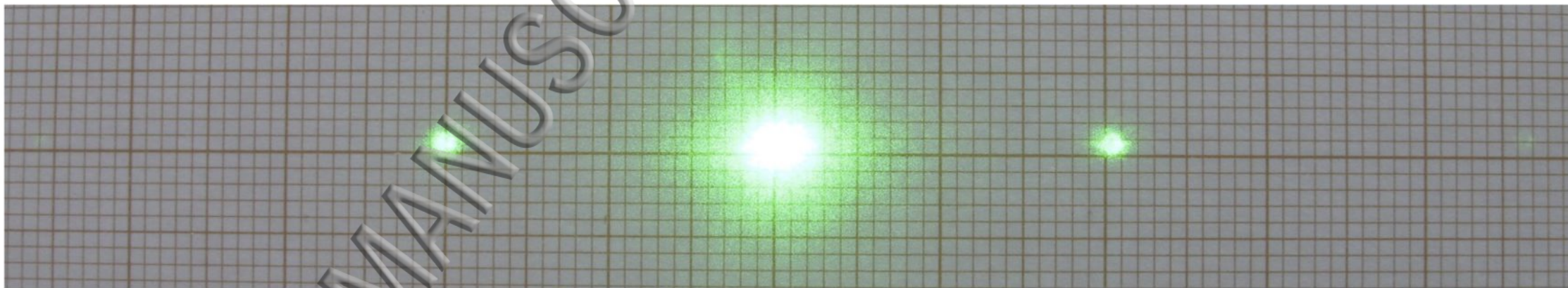
Ionogel layer
PAA sacrificial layer



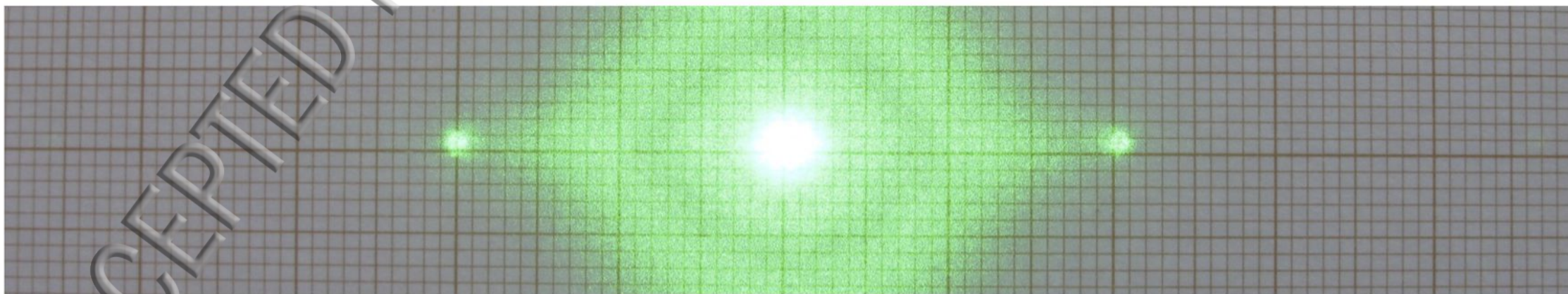
(a)



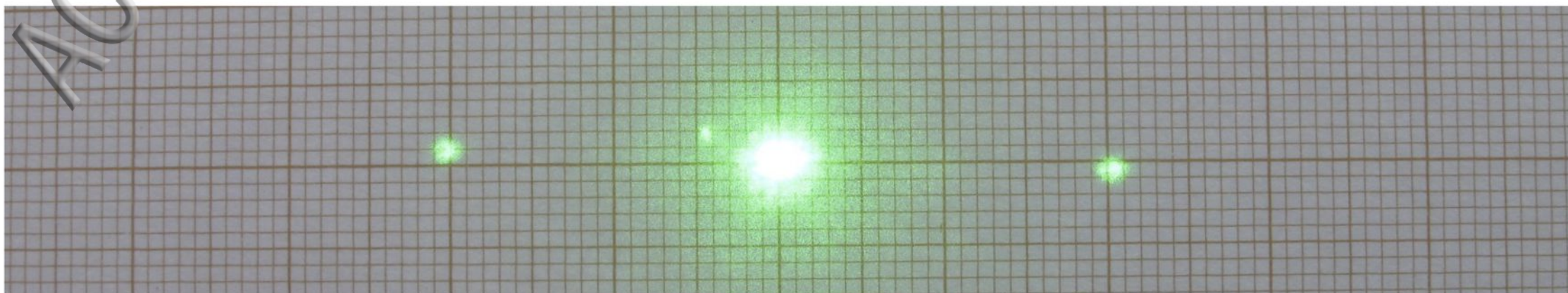
(b)

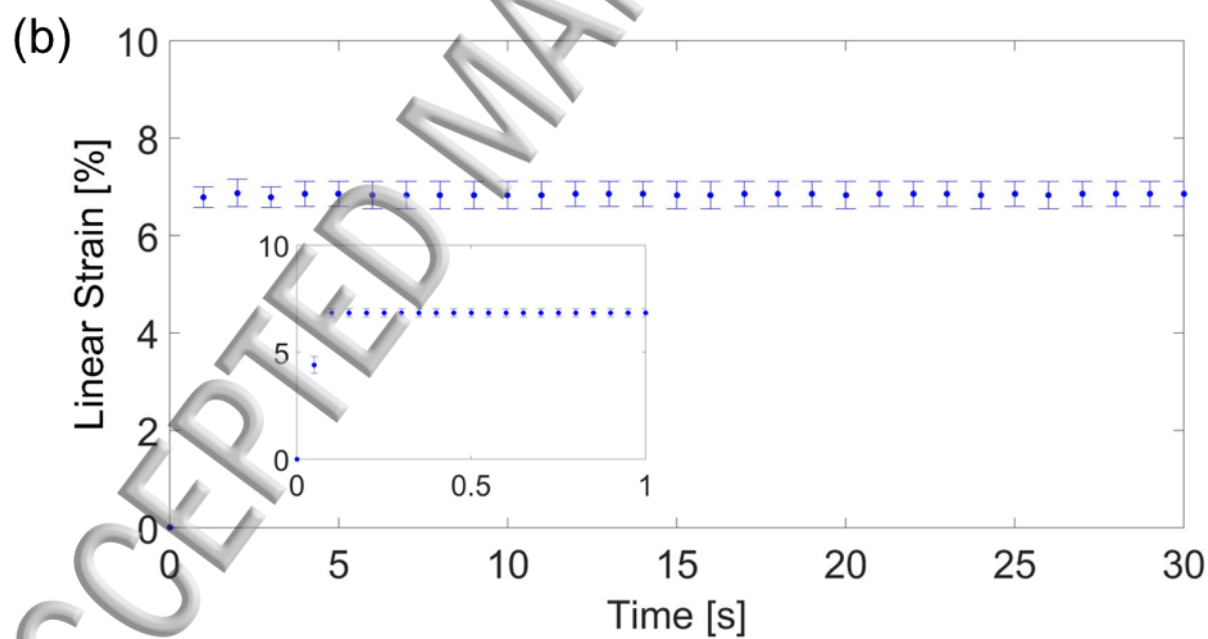
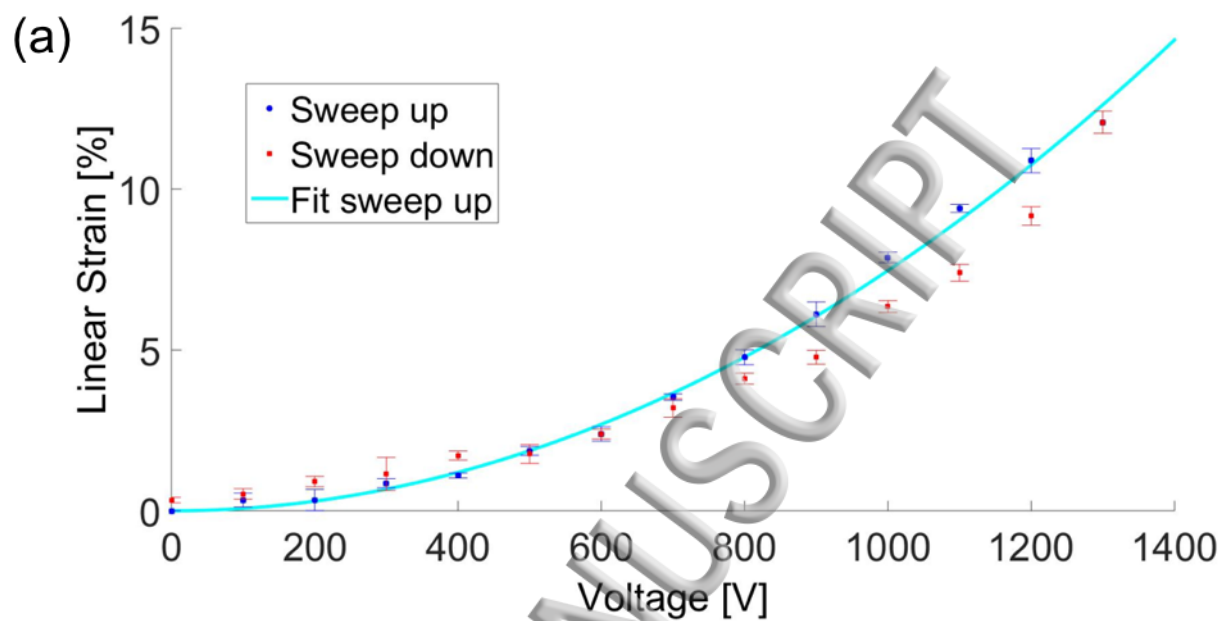


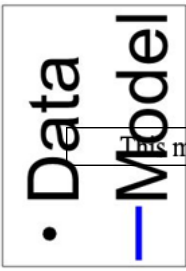
(c)



(d)







This manuscript was accepted by Appl. Phys. Lett. Click [here](#) to see the version of record.

